International Forum on Aeroelasticity and Structural Dynamics
IFASD 2022
13-17 June 2022, Madrid, Spain

PHASE RESONANCE METHOD FOR LINEARIZED IDENTIFICATION OF NONLINEAR MECHANICAL STRUCTURES

M. Tang[1], Y. Govers[1], M. Böswald[1]

[1]German Aerospace Center
Bunsenstrasse, 10, 37083 Goettingen, Germany
martin.tang@dlr.de
yves.govers@dlr.de
marc.boeswald@dlr.de

Keywords: Experimental Modal Analysis, Phase Resonance Method, Nonlinear Identification, Ground Vibration Test

Abstract: Ground Vibration Tests provide data to validate the prediction of structural dynamics of the aircraft before first flight. For this purpose, a modal substitute model is identified from experimental data. However, nonlinear dynamic behavior is often observed during those test campaigns, resulting in frequency and damping variations for specific modes. This work deals with the modal identification of aircraft with structural nonlinearities. Phase resonance method is embedded into the theory of describing functions for an improved linearized identification. Also, modal phase control is employed for automatic tuning of the excitation frequency in phase resonance testing in order to speed up the identification process. This methodology is then applied to aircraft structures and the results are discussed in the context of the assumptions made within this work. Improved results are achieved with a laboratory structure, while limits of this method are found with a real airplane structure.

1 INTRODUCTION

Flutter is an aeroelastic instability which must be avoided for all possible flight conditions of an aircraft, ideally already considered during design phase. Usually, numerical models are utilized for aeroelastic stability assessment which comprise e.g. FEM for structural dynamics and CFD for unsteady aerodynamic forces. The model predictions must be verified with test data before the first flight of the aircraft prototype. Hence, a ground vibration test (GVT) is conducted in order to identify the actual modal data from the acquired vibration data. Eigenfrequencies and mode shapes from test can be compared against the numerical model. During GVT, nonlinearities often occur [1, 2]. For accurate validation, these nonlinearities have to be detected and also characterized within a tight time schedule. Currently, DLR applies swept sine excitation and the virtual driving point method (SVDP) in case of 2 or more simultaneous excitation points [3] at different force levels in order to detect nonlinearities. In a second step, the estimated FRFs from those force levels are evaluated separately with linear modal analysis. Afterwards, changes of the modal parameters can be tracked as a function of force or deflection amplitude [4]. Such nonlinearity plots are referred to as backbone curve. Two main observations can be made during a GVT. First, only a small subset of modes will show nonlinear behavior. Second, swept sine excitation can lead to significantly distorted resonance peaks in the FRF measurement, if nonlinearities exist. In this case, the accuracy of linear modal analysis methods is limited, which has a direct impact on the quality or even validity of the identified backbone curves.

Nevertheless, linear methods are robust and readily available in different commercial software packages. With the approach for linearized identification of nonlinear systems, we want to retain the linear identification techniques for nonlinear characterization of single modes. In order to do so, the structure is linearized at different response amplitudes and modal properties are identified. One possibility for linearization of nonlinear systems is harmonic linearization and can be implemented experimentally within phase resonance method (PRM). This method delivers reasonable results, at least for eigenfrequency and mode shape vector, but is time consuming in application and requires mode isolation by force appropriation. It shall be pointed out, that new technologies are available in the meantime to automate the frequency adjustment in PRM. This potentially reduces the testing time for nonlinear identification of the modes of interest.

In the following, the theoretical framework is described for linearization of nonlinear structures. Then, the presented methodology is applied to a laboratory structure and a real aircraft structure. Finally, the difference of the results between laboratory and real aircraft structure is discussed.

2 THEORETICAL BACKGROUND

Harmonic balance allows linearization for nonlinear systems with sinusoidal input. Nonlinear systems will respond with higher harmonics if excited with a pure sine wave. In order to linearize the system, higher harmonics are neglected and only the fundamental harmonic is taken. The input output relation between the fundamental harmonic of the response and of the input results in the linearized system. [5]

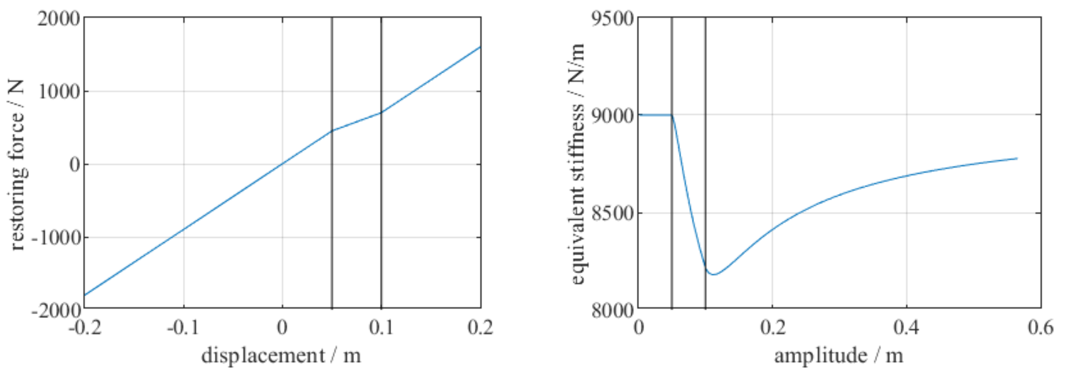

(a) restoring force for bilinear stiffness (b) linearized stiffness for different amplitudes

Figure 1: Harmonic balance for piecewise linear stiffness.

An illustrative example is shown in Figure 1. The left side shows the restoring force for a piecewise linear stiffness, which represents a gap. After $0.05\,\mathrm{m}$ the stiffness reduces and after $0.1\,\mathrm{m}$ the stiffness returns back to its original value. The right side shows the linearized stiffness for different amplitudes. The linearized or equivalent stiffness remains constant until the amplitude is reached at which the stiffness reduces. Then the equivalent stiffness drops until the amplitude reaches $0.1\,\mathrm{m}$. Afterwards, the equivalent stiffness increases again until it converges towards the original stiffness.

An experimental implementation of harmonic balance can be achieved with PRM, where sinusoidal excitation is applied. The theory of PRM is briefly reviewed hereafter. The equation of motion for a linear system with sinusoidal input reads

$$-\omega^2 [M] \{\hat{x}\} \sin(\omega t) + \omega [D] \{\hat{x}\} \cos(\omega t) + [K] \{\hat{x}\} \sin(\omega t) = \left\{\hat{F}\right\} \sin(\omega t + \phi) \quad . \quad (1)$$

If the external force compensates the internal damping forces, Equation (1) turns into

$$\left(-\omega^2 [M] + [K]\right) \{\hat{x}\} \sin(\omega t) = \{0\} \qquad . \tag{2}$$

Equation (2) is the solution of the undamped eigenvalue problem. The excitation frequency equals the eigenfrequency and the structure is vibrating in its mode shape, i.e. all other mode shapes are suppressed and single degree of freedom (SDOF) methods are applicable for identification. [6]

Since damping forces are phase shifted by $90°$ and canceled by excitation forces, the phase shift from external force to response must be $90°$ as well, which is the phase resonance criterion. An experimental implementation of harmonic balance is achieved if higher harmonics are neglected. Modal parameters are identified with stepped sine excitation around the resonance frequency. Looking at Figure 1, the linearized parameters are changing with response amplitude. If the excitation force is held constant, the response amplitude will reduce if excitation frequency is moved out of resonance frequency. For better linearized results, the response amplitude must be held constant by varying the excitation force [7–10].

The phase resonance criterion for a MDOF system can be evaluated as mode indicator function (MIF) according to Breitbach [11]

$$\mathrm{MIF} = 1000 \left(1 - \frac{|\Re\{\hat{x}\}| \, |\{\hat{x}\}|}{\{\hat{x}\}^H \{\hat{x}\}}\right) \qquad . \tag{3}$$

Equation (3) is maximized when real part of the response becomes zero, which means that the response is $90°$ phase shifted to excitation force.

Recently, the so called phase locked loop control (PLL) has been implemented for identification of nonlinear mechanical structures [12]. The phase shift between excitation and response signal is controlled by varying the excitation frequency. Thus, the phase resonance criterion can be commanded and the controller finds the eigenfrequency accordingly. However, the controller works for single input single output (SISO) systems only. Modal control is employed in order to extend this method for multiple input and multiple output (MIMO) systems. Two vectors are chosen, in order to blend the input of the controller as a single virtual output of the responses, i.e. the modal response of the structure, on the one hand and another vector is chosen in order to distribute one single virtual output of the controller, i.e. the modal excitation force, to the attached shakers. The two vectors are chosen such that the response is reduced to one modal coordinate and the excitation is exciting one single mode. [13]

Now, the link from modal phase control to the phase resonance criterion is established. For a linear system, the optimal modal filter is given by [14]

$$\{v^\mathsf{T}\} = \{\varphi^\mathsf{T}\} [M] \qquad , \tag{4}$$

with $\{\varphi\}$ being the mode shape under investigation and $\{v\}$ the blending vector. The implemented PLL in this work uses the $\tan$ function to estimate the phase, which means that the phase for the virtual output q is computed as $\tan\phi = \Re(q) / \Im(q)$, where the virtual output is computed as $q = \{v^\mathsf{T}\}\{q\}$. The response amplitude equals the mode shape at resonance $\{\hat{x}\} \approx \{\varphi\}$, which yields following equation

$$\begin{aligned} \tan\varphi &= \frac{\Im\left(\{\varphi^\mathsf{T}\} [M] \{\hat{x}\}\right)}{\Re\left(\{\varphi^\mathsf{T}\} [M] \{\hat{x}\}\right)} \quad \text{, with } \{\hat{x}\} \approx \{\varphi\} \\ \cot\varphi &= \frac{\Re\left(\{\hat{x}^\mathsf{T}\} [M] \{\hat{x}\}\right)}{\Im\left(\{\hat{x}^\mathsf{T}\} [M] \{\hat{x}\}\right)} \qquad . \end{aligned} \tag{5}$$

Equation (5) shows that the PLL controller tunes a value similar to MIF from Equation (3). If phase lag is controlled to $90°$ the value goes to zero, which maximizes the MIF value. The parameter being tuned in this control is the excitation frequency. Equation (5) is similar to the MIF formulation from Deck [7], which is $\sum \Re(\hat{x}) / \sum \Im(\hat{x})$

For proper linearization, only the fundamental harmonic is considered for the phase estimate. From Figure 1, one can see, that the linearized stiffness varies with response amplitude. If force is kept constant at different frequencies around resonance, the response amplitude varies as well, so that the linearized stiffness value also varies. The response amplitude should be kept constant rather than the force amplitude for better linearized identification [7]. In this work, an additional controller is employed for keeping response amplitude constant. The virtual response amplitude is estimated and the force signal is controlled to keep virtual response at a constant level. To the knowledge of the authors, this combination of PLL including modal extension for MIMO systems and constant response amplitude control for linearization is a novel approach. This methodology has been applied to two test cases described in the next section. The major goal is the application in future GVT for improved modal identification.

3 LABORATORY STRUCTURE

3.1 Test setup

The proposed method is applied to an aircraft like laboratory test structure at DLR called AIRMOD, as shown in Figure 2. This structure is a replica of the Garteur SM-AG19 test bed with well known dynamics, also described in literature [15, 16].

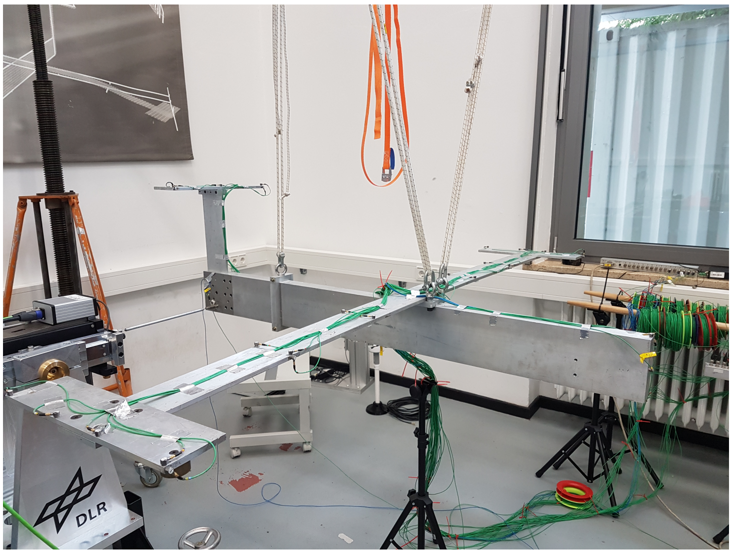

Figure 2: Laboratory structure AIRMOD.

For this test setup, a modified APS shaker is attached span wise at the back of the fuselage for excitation and 36 accelerometers are placed on the structure for measurements, as depicted in Figure 3.

From previous measurements, a detailed modal identification is available. A selection of modes are shown in Figure 4, consisting of the first and second wing bending as well as the scissors mode. The scissors mode describes an in-plane bending of fuselage and wings, resulting in a movement similar to the movement of a scissor. The corresponding modal properties are presented in Table 1. It is known that the scissors mode behaves in a nonlinear way [17] and is investigated in more detail during this study.

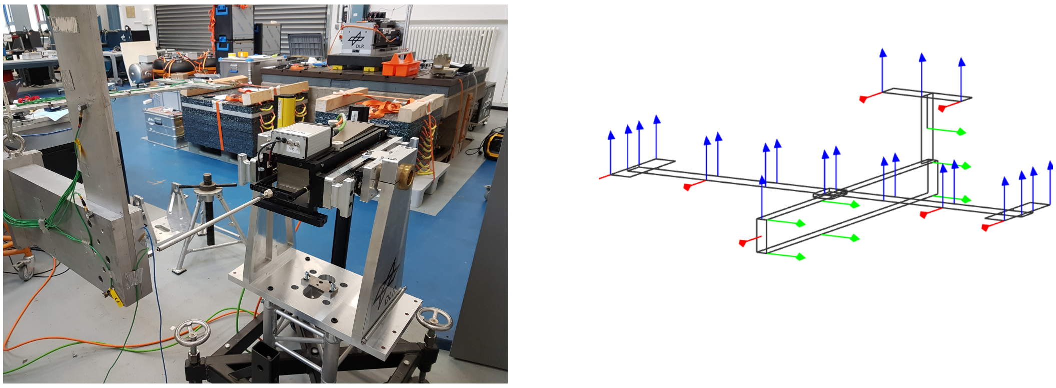

(a) close up of airplane tail (b) sensor positions

Figure 3: Exciter and sensor positions for AIRMOD.

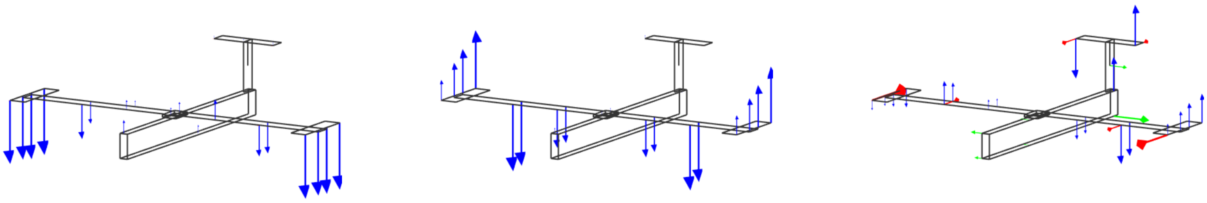

(a) wing bending (b) 2nd wing bending (c) scissors

Figure 4: Different mode shapes for AIRMOD.

Table 1: Modal properties of shown modes.

Mode	Description	f / Hz	D / -
-	wing bending	5.55	0.002
-	2nd wing bending	44.41	0.002
-	scissors	47.56	0.002

3.2 Results

A reference data set is measured by applying the methodology described by Stephan et al. [2]. Hence, structure is excited by swept sine excitation with different force levels. Figure 5 shows the computed FRFs from swept sine excitation. The peak around $47\,\mathrm{Hz}$ varies with increasing force level, indicating the nonlinear behavior of the mode, while the other peaks remaining the same for all load levels. This shows, that only one mode within the shown frequency band behaves nonlinear. Additionally, it can be seen that the peak of the FRF is distorted significantly. It is assumed that linear identification methods will lead to uncertain modal results.

In a second step, the PLL control with constant response amplitude control has been applied in order to measure linearized FRFs for improved modal identification. The half-power bandwidth for a one degree of freedom system ranges approximately from $45°$ to $135°$. So, the phase has been set to $135°$, $120°$, $90°$, $60°$ and $45°$, in order to assure measurement of 5 points within the half-power bandwidth. The following identification process can be done with simple SDOF

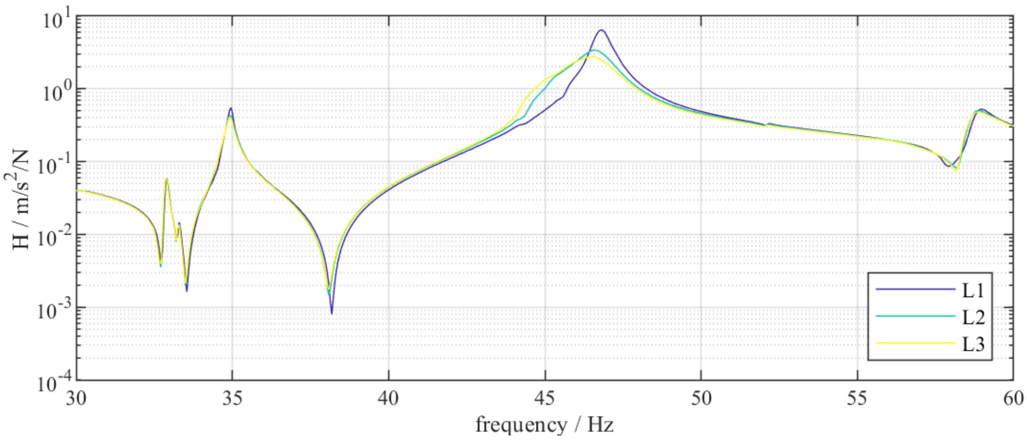

Figure 5: FRFs of SVDP for different load levels. L1: 16.46 N, L2: 36.21 N, L3: 43.89 N.

algorithms or other methods used within PRM. Clearly, the resonance also shifts down with increasing force level. However, the newly measured FRFs from stepped sine excitation are not distorted anymore due to the constant response amplitude control. Improved linear identification is expected for this data set. As reference for the FRFs, the force current from the shaker has been chosen, since control with a direct force measurement was not possible. The force levels applied here are not directly comparable to swept-sine excitation, because response amplitude with stationary sine excitation is generally higher. Further, force amplitude must be increased in order to control constant response amplitude for out of resonance points. Approximately 40 % more force is needed to retain the response amplitude at the half-power bandwidth. The applied force in resonance during this measurement is 1 N, 3 N, 7 N, 13 N and 21 N.

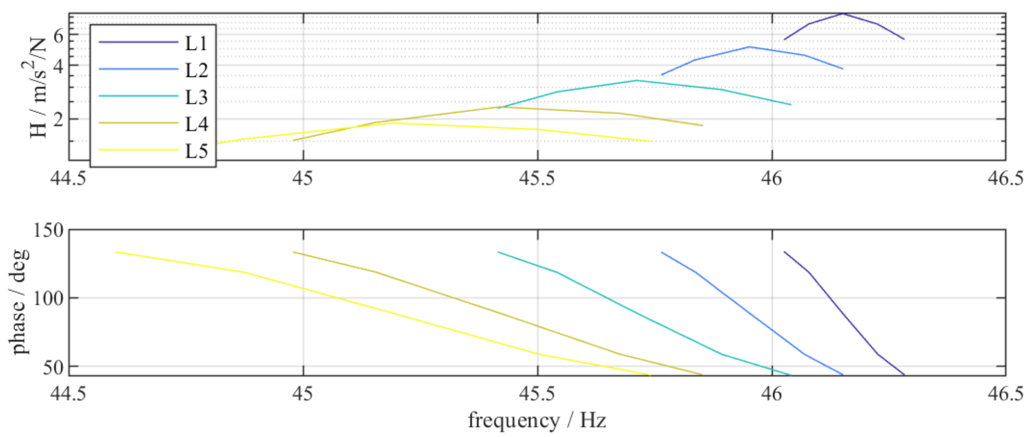

Figure 6: FRFs of SVDP for different load levels. L1: 1 mm, L2: 2 mm, L3: 3 mm, L4: 4 mm L5: 5 mm.

4 DO728

4.1 Test Setup

At the DLR Goettingen site, a Do728 aircraft exist for cabin testing. The Do728 aircraft was designed as a short and medium range aircraft for up to 70 passengers. The wingspan is 27 m and the empty weight is supposed to be 20.4 t. This prototype aircraft has been purchased after the manufacturer filed insolvency. Unfortunately, the wings have been cut off for transportation purposes but are reattached and supported additionally. Figure 7 shows the aircraft at DLR.

Due to the modifications, the dynamic behavior is not representative anymore, however, the applicability of this method for real aircraft can be investigated.

Figure 7: Do728 at DLR.

It has been observed in the past that mode shape participation of the tail often lead to nonlinear behavior. For this test, the horizontal tail plane (HTP) and elevator have been instrumented with accelerometers. The elevator is fixed in horizontal position. Four sections with 3 measurement points each (2 on the HTP and 1 on the elevator), are implemented on both sides. All measurement points are equipped with an accelerometer measuring out of plane. Additionally the measurement point at the leading edge of the outer section is instrumented for measurement in three directions, as depicted in Figure 8.

For excitation, two Prodera shakers, which are mounted on towers, were attached to the outer part of the HTP perpendicular to the plane, as depicted in Figure 8(a). This configuration enables the excitation of the roll mode of the tail, which will be investigated in detail, especially since the empennage is focus of the research and this has not suffered from modification.

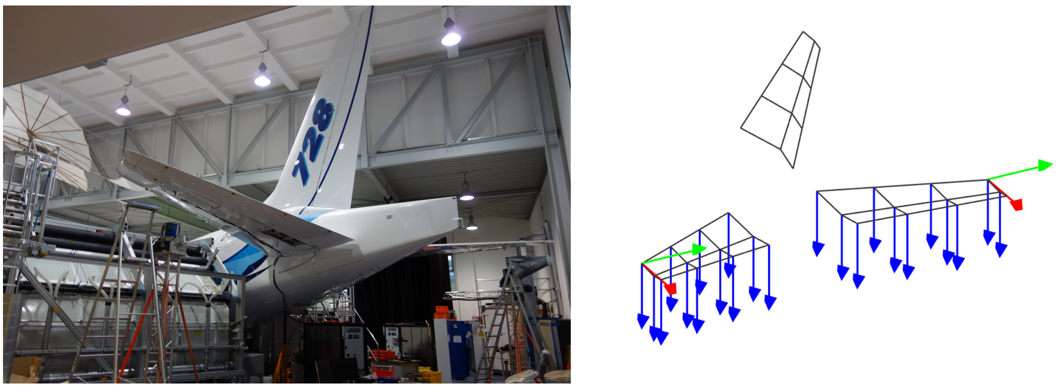

(a) Close up of airplane tail

(b) Sensor positions

Figure 8: Tail of aircraft and sensor positions.

4.2 Results

For an overall overview of the dynamic behavior, a broad band random excitation has been applied. The resulting driving point FRFs for left and right side are illustrated in Figure 9. The FRFs differ a little, which indicates that the structure is not symmetric. The attachment of the shakers are also not exactly symmetric due to different conditions of the ground, where the shaker tripods are standing on.

Modes are estimated with the pLSCF algorithm [18]. The interpretation of modes is difficult since only the tail is instrumented while other components are not observed. Three arbitrary mode shapes are depicted in Figure 10. The first mode shows a rolling of the tail (Figure 10(a)), which will be investigated in detail. Figure 10(c) represents a HTP bending, where two nodes are clearly seen. In contrast to the HTP bending, no nodes are seen in Figure 10(b). This indicates a movement of the fuselage, showing possibly a fuselage bending. The corresponding values for eigenfrequencies and damping are shown in Table 2 However, the identification of this aircraft is not of interest but the applicability of the proposed method with a real world demonstrator.

Table 2: Modal properties of shown modes.

Mode	Description	f / Hz	D / -
1	HTP roll	5.67	0.02
2	fuselage bending	7.19	0.01
9	HTP bending	13.96	0.01

Again, a reference data set is measured first. Hence, sweep runs have been made with two shakers, where the signal was shifted by 180°, in order to excite anti-symmetric modes only, where the rolling of HTP is of special interest. Due to the correlated nature of the excitation signal, SVDP has been utilized to compute FRFs [3]. Different force levels have been used, in order to observe the change in eigenfrequency. If the mode was linear, no change would be observable. Figure 11 shows FRFs for the virtual driving point and a decreasing frequency for the peak with increasing force level is observed.

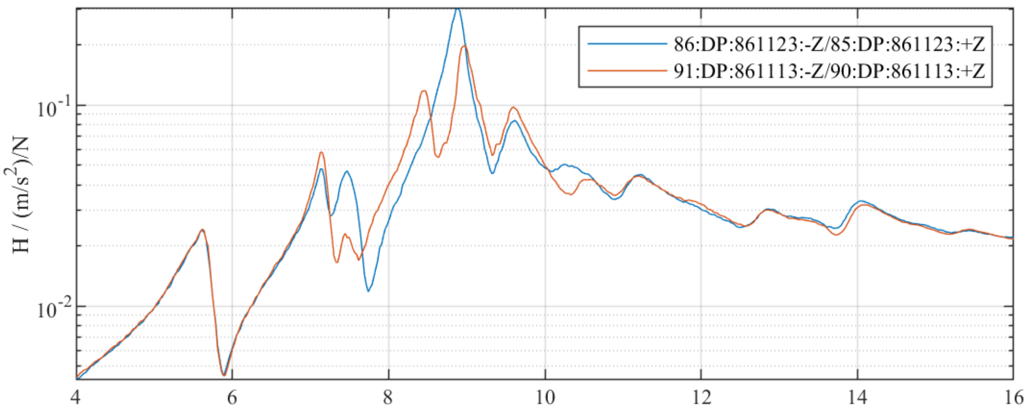

Figure 9: FRFs of driving point accelerometers for excitation at 80% wingspan of the HTPs with a random signal.

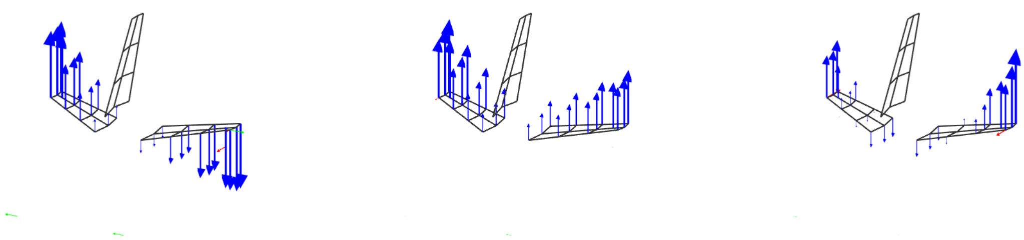

(a) Mode 1 (b) Mode 2 (c) Mode 9

Figure 10: Mode shapes for Do728.

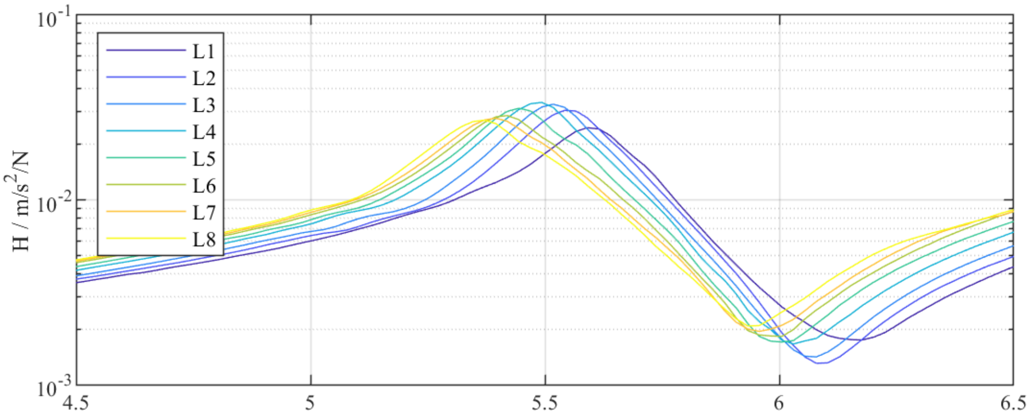

Figure 11: FRFs of SVDP for different load levels. L1: 7.53 N, L2: 15.05 N, L3: 22.57 N, L4: 37.62 N, L5: 52.66 N, L6: 75.23 N, L7: 90.28 N, L8: 105.33 N.

In the following, PLL control with constant response amplitude has been applied for modal identification. Figure 12 plots the result for different load levels. In this case, load levels were set as constant amplitude for the virtual response. The phase has been set to $-73°$, $-78°$, $-84°$, $-90°$, $-96°$, $-102°$ and $-107°$ for each measurement run and the response amplitude has been set to $1\,\mathrm{mm}$, $1.5\,\mathrm{mm}$ and $2\,\mathrm{mm}$. In contrast to the first case, phase range has been modified because the controller failed for a commanded phase lag of $-135°$. Thus, the range of the phase has been reduced. It is seen that the maximum response is not at $-90°$. The single degree of freedom assumption doesn't hold anymore. Also for the highest load level, the shape of the FRF does look distorted. A sudden jump around $5.45\,\mathrm{Hz}$ for the L3 measurement is seen. Higher response amplitude levels could not be controlled anymore, so the measurements were stopped after this response level.

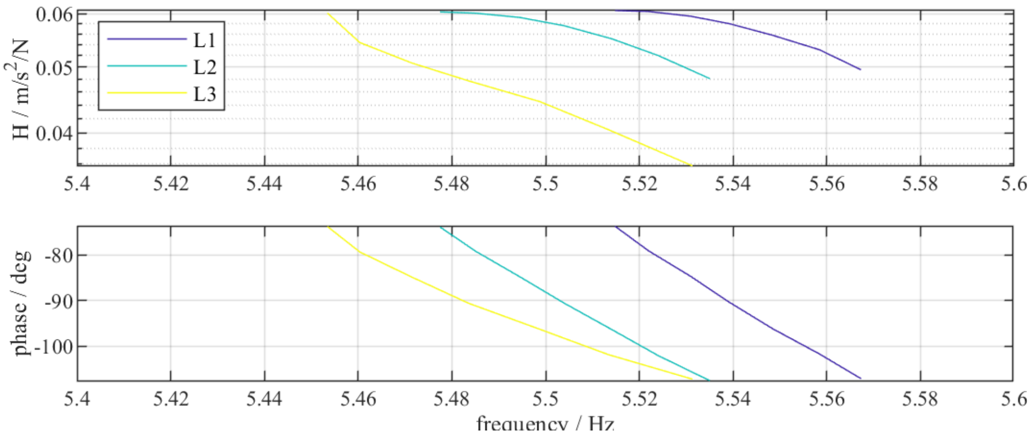

Figure 12: FRFs of SVDP for different load levels. L1: $1\,\mathrm{mm}$, L2: $1.5\,\mathrm{mm}$, L3: $2\,\mathrm{mm}$.

5 DISCUSSION

Two test cases are investigated with the proposed method for improved linear identification. Good results are obtained for the laboratory structure. The linearization works and FRFs shown in Figure 6 are behaving in a linear manner in comparison to Figure 5. This allows proper identification with linear methods. The measured data shows, that the eigenfrequency is decreasing with increasing force level, or also increasing response amplitude. Also, the half-power bandwidth is increasing while peak value is decreasing, indicating increasing damping. Explanation for this behavior is friction nonlinearity between wing and fuselage, which is activated, when the scissors mode is excited.

However, results from test with Do728 were not as promising as AIRMOD results. On the one hand, more shakers are used and on the other hand the modal density of the structure is much higher. Inspecting Figure 11, a transition in frequency for the peak is seen, but the shape of the FRF remains rather linear. Interestingly, the peak value of the FRF is increasing with higher force levels in the beginning but decreasing again with even higher force levels.

The HTP is connected to the fuselage with a trim spindle to control the angle of attack. A gap is needed in order to rotate HTP against fuselage. For better aerodynamics, the gap is closed with rubber sealing. Nonlinear material behavior of this sealing is assumed.

Figure 12 shows the results for the proposed method. Unfortunately, no improvement in comparison to Figure 11 is seen. Moreover, difficulties regarding the phase control have been observed. Also, at $90°$ the response amplitude is not at its peak, which is in contrast to the SDOF assumption, although a clear single peak is seen in Figures 9 and 11. In order to investigate this, a closer look at the phase from sweep measurements is taken, shown in Figure 13. The FRFs are computed with SVDP algorithm including a blending to compute virtual input and output, very similar to the proposed algorithm in this study. Phase behavior from those measurements is thus representative for the phase control. Close observation reveals that the maximum amplitude is not at $90°$ as already seen with PLL control although one distinct peak is seen. This indicates that the force appropriation was not good enough to isolate a single mode shape. Careful inspection of the response amplitude reveals an anti-resonance around $6\,\mathrm{Hz}$. This is also seen in the phase response, which increases roughly from $-120°$ to $0°$. So, the anti-resonance affects also the phase behavior of the resonance by shifting it little from $-90°$ towards increased values. The coupling between resonance and anti-resonance is stronger the higher the damping ratio of the mode is, so that assumptions for phase resonance are not hold anymore.

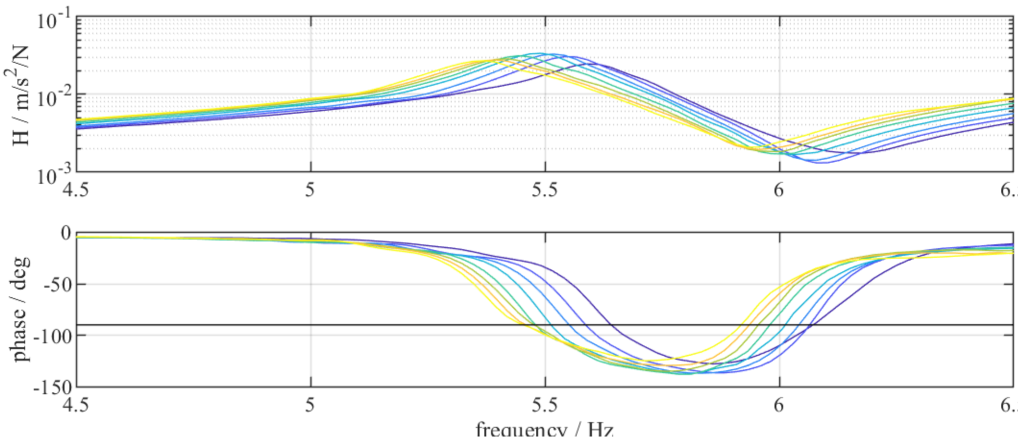

Figure 13: Phase behavior of SVDP for different load levels.

During the test, it has been observed that it is not possible to control certain phases. Looking at Figure 13, it can be seen that some phases below $-120°$ are simply never reached with this excitation around this mode. This means that the mode under investigation has not been isolated properly, although a single distinct peak is seen for the FRF in Figure 12. The anti-resonance which is a linear phenomenon leads to a phase distortion and thus, the phase resonance criteria doesn't hold anymore. In theory, other modes can be suppressed with more shakers. However, in practice it is very difficult, especially, because some points on the structure are not adequate or reachable for excitation.

Due to modal interaction with other modes or anti-resonances, the phase at resonance might change from $90°$ to a different value. One could think to choose a different phase as a new resonance criterion. However, due to damping variation of the nonlinear mode with increasing response amplitude levels, the interaction with other modes also changes and hence, the new resonance criterion is affected as well. Since the SDOF assumption of the FRF at its resonance does not hold, the processing for identification must be adapted as well.

In the end, this means that only modes can be isolated and identified, if the FRF from sweep run shows a clear SDOF behavior in amplitude and especially in phase. Otherwise new exciter configurations are needed or another methodology needs to be applied.

6 CONCLUSION

A method has been proposed for identification of nonlinear mechanical structures, based on phase resonance. A modal phase controller has been employed for faster tuning and enables application for MIMO systems.

Two test cases are used to assess this approach. The aircraft like laboratory structure AIRMOD has been excited with a single shaker with promising results. Then, the approach has been tested on a real aircraft structure, where the limits of this approach were shown. An anti-resonance distorted the phase behavior, such that the phase resonance criterion does not hold anymore. The limits of classical phase resonance, which has been observed in the past are still challenging. More shakers could be used in theory in order to suppress modes, which are not of interest. However, due to limited possible positions for excitation and also limited number of shakers this remains an unsolved issue.

Nevertheless, the proposed method has been applied successfully on a laboratory structure. The reasons why it does not work properly on the more complex structure is discussed, such that a prognosis can be given after first measurements, if this approach is feasible or not.

7 REFERENCES

[1] Lubrina, P., Giclais, S., Stephan, C., et al. (2014). Airbus a350 xwb gvt: State-of-the-art techniques to perform a faster and better gvt campaign.

[2] Stephan, C., Lubrina, P., Sinske, J., et al. Airbus beluga xl state-of-the-art techniques to perform a ground vibration test campaign of a large aircraft. In *IFASD 2019*.

[3] Fuellekrug, U., Boeswald, M., Goege, D., et al. (2008). Measurement of frfs and modal identification in case of correlated multi-point excitation. *Shock and Vibration*, 15(3-4), 435–445.

[4] Gloth, G. and Sinapius, M. (2004). Influence and characterisation of weak non-linearities in swept-sine modal testing. *Aerospace Science and Technology*, 8(2), 111–120.

[5] Gelb, A. and Vander Velde, W. E. (1968). *Multiple-input describing functions and nonlinear system design*. McGraw-Hill electronic sciences series. New York u.a.: McGraw-Hill.

[6] Wright, J. R., Cooper, J. E., and Desforges, M. J. (1999). Normal-mode force appropriation—theory and application. *Mechanical systems and signal processing*, 13(2), 217–240.

[7] Fillod, R. (1982). Some identification methods using measured harmonic responses. In H. G. Natke (Ed.), *Identification of Vibrating Structures*. Vienna: Springer Vienna, pp. 121–145.

[8] Tanrikulu, O., Kuran, B., Ozguven, H. N., et al. (1993). Forced harmonic response analysis of nonlinear structures using describing functions. *AIAA Journal*, 31(7), 1313–1320.

[9] Link, M., Boeswald, M., Laborde, S., et al. (2011). An approach to non-linear experimental modal analysis. In T. Proulx (Ed.), *Nonlinear Modeling and Applications, Volume 2*, Conference Proceedings of the Society for Experimental Mechanics Series. New York, NY: The Society for Experimental Mechanics Inc, pp. 119–128.

[10] Karaağaçlı, T. and Özgüven, H. N. (2021). Experimental modal analysis of nonlinear systems by using response-controlled stepped-sine testing. *Mechanical systems and signal processing*, 146, 107023.

[11] Breitbach, E. (1974). A semi-automatic modal-survey test technique for complex aircraft and spacecraft structures. *1974*, 519–528.

[12] Peter, S. and Leine, R. I. (2017). Excitation power quantities in phase resonance testing of nonlinear systems with phase-locked-loop excitation. *Mechanical systems and signal processing*, 96, 139–158.

[13] Tang, M., Stephan, C., and Böswald, M. Phase resonance method for nonlinear mechanical structures with phase locked loop control. In *ISMA 2020*.

[14] Balmes, E. (2018). Shapes & dof: on the use of modal concepts in the context of parametric non-linear studies. In *ISMA*.

[15] Govers, Y. (2012). *Parameter identification of structural dynamic models by inverse statistical analysis*. Ph.D. thesis, Kassel, Univ., Fachbereich Bauingenieur- und Umweltingenieurwesen.

[16] Link, M. and FRISWELL, M. (2003). Working group 1: Generation of validated structural dynamic models - results of a benchmnark study utilising the garteur sm-ag19 test-bed. *Mechanical systems and signal processing*, 17(1), 9–20.

[17] Govers, Y., Boebswald, M., Fuellekrugn, U., et al. Analysis of sources and quantification of uncertainty in experimental modal data. In *ISMA 2006*. pp. 4161–4173.

[18] Guillaume, P., Verboven, P., Vanlanduit, S., et al. (2003). A poly-reference implementation of the least-squares complex frequency-domain estimator. In *Proceedings of IMAC*, vol. 21. pp. 183–192.